

Revisiting Epithelial-to-mesenchymal Transition through Adenoid Cystic Carcinoma

AMANDA SIU, CASEY LEE, ERIC PHAM and DANIEL M. RAMOS

*Department of Orofacial Sciences, University of California at San Francisco,
San Francisco, CA, U.S.A.*

Abstract. Adenoid cystic carcinoma (ACC) has a 5-year survival rate of 90%. The 15-year survival rate drops to 10% due to recurrence and invasion. ACC has three subtypes: cribriform, tubular, and solid. The cribriform subtype has the best prognosis and the solid subtype has the worst prognosis. By immunohistochemistry of tissue sections, we showed that the solid form expresses $\alpha\beta6$ integrin and tenascin-C, which are known promoters of epithelial-to-mesenchymal transition (EMT). We also defined two ACC cell lines with the characteristics of the cribriform and solid subtype. The SACC83 cells grow in basaloid-like clusters and express high levels of E-cadherin. In contrast, the ACCch cells are more myoepithelial-like and express high levels of vimentin and of $\alpha\beta6$ integrin. The ACCch cells are highly invasive and this behavior is dependent upon the $\alpha\beta6$ integrin function. Our results suggest that the transition from the cribriform to solid form may occur through EMT.

Adenoid cystic carcinoma (ACC) is the most common malignancy of the minor salivary glands and accounts for 25% of all salivary gland tumors (1). It is relatively slow-growing yet highly invasive with a high rate of recurrence (2). Distant metastasis frequently occurs despite loco-regional tumor control and this can occur more than ten years after initial therapy (2). The majority of patients with ACC survive 5 years post-surgery and radiation therapy. The 15-year survival rate drops to 10% (3).

Histologically, ACC has three major subtypes: cribriform, tubular and solid. The most common subtype

is cribriform. The cribriform pattern is well-differentiated and has an excellent prognosis. It is composed of basaloid cell islands surrounding cyst-like spaces (4). The tubular pattern is characterized by glandular spaces of elongated tubules lined by epithelial cells, surrounded by single or multiple layers of basaloid cells (4). The solid pattern is poorly-differentiated, very aggressive, and has the worst prognosis. The solid subtype is composed of solid tumor islands with necrosing centers (4). The cribriform subtype represents a highly-differentiated form of the disease, which converts to the poorly-differentiated solid form of the disease. The mechanism of transitions between the ACC subtypes is not understood. Our work suggests that the process involves a loss of differentiation. This transition underlies the high morbidity and mortality associated with this disease (5).

To fully understand tumor cell invasion and metastasis, it is important to understand the tumor microenvironment and how the cells interact with the extracellular matrix (ECM) (6). The main receptors mediating attachment to the ECM are the integrin family of adhesion molecules. Integrin binding triggers a variety of intracellular signaling pathways. The $\alpha\beta6$ integrin is an epithelial-specific receptor for ECM components such as, fibronectin (FN), tenascin (TN-C), and also activates transforming growth factors $\beta1$ and $\beta3$ (TGF $\beta1$ and TGF $\beta3$) (7). The interactions between integrins and the ECM are important for tumorigenesis, invasion, and metastasis. Tenascin-C (TN-C) is a large glycoprotein prominent in the ECM of specific embryonic tissues, healing wounds, and tumors (8). TN-C has been shown to promote tumor cell proliferation, tumor cell migration, and epithelial-to-mesenchymal transition (EMT) (8). Previous studies showed that tumor cells undergoing $\alpha\beta6$ integrin-induced EMT secrete TN-C (9).

Previous studies from our laboratory demonstrate that the expression of the integrin $\alpha\beta6$ promotes the epithelial-to-mesenchymal transition (EMT) and metastasis in a variety of epithelial tumors including oral squamous cell carcinoma (SCC) (9). In this study, we investigate whether EMT

Correspondence to: Daniel M. Ramos, DDS, Ph.D., Department of Orofacial Sciences, University of California, 513 Parnassus Ave, S612, Box 0422, San Francisco, CA 94143-0422, U.S.A. Tel: +14155024905, Fax: +18007836653, e-mail: Daniel.ramos@ucsf.edu

Key Words: Adenoid cystic carcinoma, ACC, epithelial-to-mesenchymal transition, EMT, $\alpha\beta6$, invasion, SACC83, ACCch cells.

regulates the transition of ACC from the cribriform state to the solid state through monitoring the expression of EMT markers $\alpha\beta6$ and TN-C.

Materials and Methods

Cell culture. The SACC83 and ACCh cell lines were derived from two sublingual gland tumors and were generous gifts from Dr. Osama Tetsu (University of California, San Francisco). The SACC83 cells are routinely cultivated in Dulbecco's modified Eagle's medium (DMEM) with 10% fetal bovine serum (FBS). ACCh cells are grown serum-free in Keratinocyte Growth Medium (KGM). Both cell lines are grown at 37°C with 5% CO₂ and 95% humidity. The conditioned medium used as a chemoattractant was produced by serum-starving peritumor fibroblasts for 72 h. The media was collected, sterile filtered and used in the invasion assay.

Reagents. Mouse monoclonal anti-integrin $\beta6$ antibody, clone CS $\beta6$, was purchased from Millipore (Billerica, MA, USA). Mouse monoclonal function blocking antibody 10D5 was a generous gift from Dr. Dean Sheppard (UCSF). Mouse monoclonal antibodies to tenascin-C (BC-4) were kindly provided by Luciano Zardi (Istituto Nazionale, Genoa, Italy). Mouse monoclonal antibodies against vimentin (clone 3B4) and against actin (mAb 3128) were purchased from Chemicon International (Temecula, CA, USA). Rabbit polyclonal antibodies to cytokeratin and anti-E-cadherin antibodies (clone She-78-7) were from Zymed Laboratories (South San Francisco, CA, USA). Monoclonal antibodies to the phosphorylated Fyn were from Santa Cruz Biotechnology (Santa Cruz, CA, USA).

Immunofluorescence microscopy. A total of 2×10^5 cells/ml were plated onto uncoated glass coverslips (10 $\mu\text{g}/\text{ml}$) serum-free for 24 h, fixed with 2% paraformaldehyde and permeabilized with 0.1% Triton[®] X-100. The cells were incubated with anti-mAb for 1 h and rinsed with phosphate-buffered saline (PBS). The cells were then incubated with goat anti-mouse or anti-rabbit IgG conjugated to fluorescein isothiocyanate (FITC) for 30 min at room temperature. Coverslips were mounted with Vectashield (Vector Laboratories, Burlingame, CA, USA). Cells were imaged using a Nikon 80i immunofluorescence microscope.

Western blotting. The cells were serum-starved for 24 h and then plated onto fibronectin (10 $\mu\text{g}/\text{ml}$) for 24 h. The cells were then lysed in Nonidet P-40 lysis buffer (1.4% Nonidet P-40, 150 mM NaCl, 0.2% SDS, 1 mM EDTA, 20 mM Tris-HCl, 1 mM phenylmethylsulfonyl fluoride, 10 $\mu\text{g}/\text{ml}$ leupeptin, 10 $\mu\text{g}/\text{ml}$ aprotinin, 1 mM Na₃VO₄, 50 mM NaF). The proteins were separated by SDS-membrane (Micon Separation Inc, Westborough, MA, USA) using a semi-dry blotting apparatus (Bio-Rad, Hercules, CA, USA), as previously described. ECL (Amersham; Piscataway, NJ, USA) developed the membranes. The blots were quantified and assigned relative value units (rvu) using an image analysis program (NIH Image, <http://www.rsb.info.nih-image>). The bands were quantified from exposures that placed them within the linear range of the film.

Invasion assay. The upper surface of Biocoat[®] membranes (for 24 well plates with pore size 8 μm , BD Falcon) are coated with 10 $\mu\text{g}/\text{ml}$ Matrigel or poly-d-lysine. A total of 2×10^5 cells/ml were plated into each insert and 400 μl of peritumor fibroblast (PTF) conditioned

medium (CM) was used as a chemo-attractant in the lower chamber. The cells were allowed to migrate at 37°C for 24 h. Cells that did not migrate through the pores in the membrane were removed by scraping the membrane with a cotton swab. The cells that migrated through were stained with crystal violet. In order to quantify the migration, cells in ten random fields of view at $\times 100$ were counted and expressed as the average number of cells/field of view. Three independent experiments were performed in each case.

Results

$\alpha\beta6$ and TN-C are differentially expressed in the different adenoid cystic carcinoma. Tissue sections of ACC were incubated with antibodies against $\beta6$ and TN-C, both of which are known promoters of EMT. When processed for immunohistochemistry, we found that the cribriform subtype expressed trace amounts of $\alpha\beta6$ integrin. The $\alpha\beta6$ integrin was localized to the cell membrane in some of the glandular type structures at the perimeter of the lesion (Figure 1; Panel A). In contrast, the solid subtype expressed $\alpha\beta6$ integrin throughout the entire lesion (Figure 1; Panel B). When the tissue was examined for expression of TN-C, protein expression was lightly identified in the connective tissue associated with the cribriform subtype (Figure 2; Panel A). In contrast, TN-C expression was detected throughout the entire lesion of the solid subtype (Figure 2; Panel B). These results show that EMT markers $\alpha\beta6$ integrin and TN-C are highly expressed in the solid form but not in the cribriform subtype.

SACC83 and ACCh cell lines represent two distinct growth patterns of ACC. The SACC83 (Figure 3 A, B) and ACCh cells (Figure 3 C, D) were grown as monolayers and photographed at pre-confluence (Figure 3; A, C) and at confluence (Figure 3 B, D). At pre-confluence, the SACC83 cells grew as tight epithelial-like nests expressing a basaloid appearance, which ultimately had a uniform cobblestone appearance at confluence (Figure 3; A, B; respectively). In contrast, the ACCh cells had a spindle shape, myoepithelial/mesenchymal appearance independent of confluence (Figure 3; C, D). These results suggest the SACC83 and ACCh may represent two extremes of ACC: epithelioid versus myoepithelial.

Expression of E-cadherin and vimentin categorize ACC cells as epithelioid or mesenchymal. The biochemistry associated with ACC morphology was examined by western blotting using antibodies to the epithelial marker E-cadherin and to the mesenchymal marker vimentin. The cells were grown under serum-free conditions for 24 h and were then lysed. The lysate was separated using SDS-PAGE and analyzed by western blotting. The membranes were scanned by dosimetry and assigned relative value units (rvu). The SACC83 cell line expressed 5 times the amount of E-cadherin than the ACCh cell line (Figure 4). Vimentin expression was the opposite.

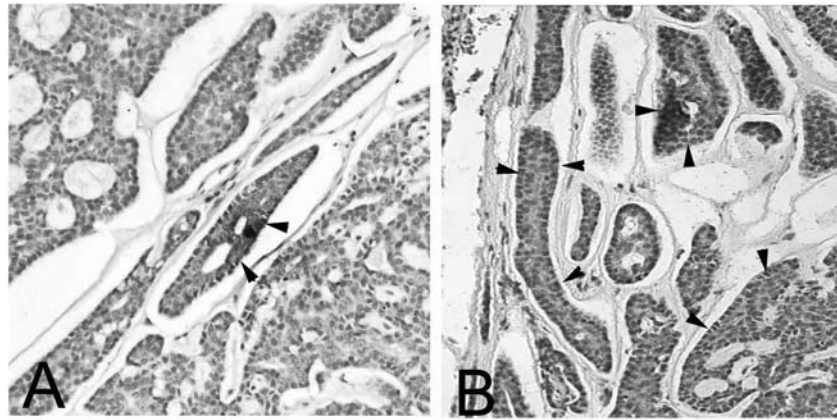


Figure 1. Differential expression of $\alpha v \beta 6$ integrin in ACC tissue sections. Tissue sections of ACC were de-parafinized and processed for immunohistochemistry. The sections were classified as either cribriform (A) or solid (B) subtype ACC. The tissue was incubated with antibodies against the $\beta 6$ (Cs $\beta 6$) integrin subunit and processed for routine histochemistry. Only one area of the cribriform tissue was positive for $\beta 6$ (see arrows); whereas the rest of the lesion was totally negative (A). When the solid tissue was evaluated the entire lesion was positive for $\beta 6$ (B, see arrows). This indicates a differential expression of $\beta 6$ when the cribriform type is compared to the solid form.

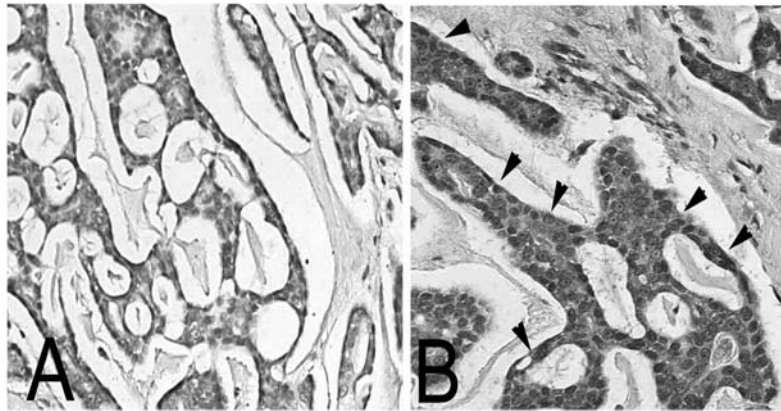


Figure 2. Differential expression of TN-C in ACC tissue sections of ACC. ACC tissues sections were next evaluated for expression of TN-C using a mouse monoclonal antibody against BC-4, which recognizes all TN-C isoforms. The tissues were incubated with the antibody and further evaluated for expression. The extracellular matrix surrounding the cribriform tissue was totally negative for TN-C expression (A). Both the extracellular matrix and the tumor cells in the solid subtype were rich in TN-C (B, see arrows). This represents a dramatic shift in the matrix associated with the two extreme subtypes of ACC.

Vimentin expression was 7 times greater in the ACCh cell line when compared to the SACC83 cell line (Figure 4). These results further characterize the SACC83 and ACCh cells as epithelial and mesenchymal, respectively. The SACC83 cells possess a well-differentiated epithelial phenotype, which is rich in E-cadherin similar to the one demonstrated by the cribriform type. The ACCh cells are more fibroblast-like and poorly differentiated similar to the solid ACC subtype.

Differential expression of $\alpha v \beta 6$ integrin and pFyn in SACC83 and ACCh. Our previous work on oral SCC showed that the expression of the $\alpha v \beta 6$ integrin promotes invasion

by conferring the mesenchymal phenotype to highly differentiated epithelial cells thus promoting EMT *via* the phosphorylation of Fyn. Fyn phosphorylation then initiates a cascade of events ultimately activating MAPK and enzymatic gene expression (10). To further evaluate this complex we used western blotting, to examine the expression of the $\alpha v \beta 6$ integrin and of phosphorylated Fyn kinase (pFyn) in the ACC cell lines. The lysate from the poorly-differentiated, ACCh cells expressed 9-fold greater amounts of $\alpha v \beta 6$ integrin than the SACC83 cells (Figure 5). The SACC83 cells had minimal expression of the $\alpha v \beta 6$ integrin and no expression of active Fyn kinase (Figure 5). These results represent a clear distinction between the two

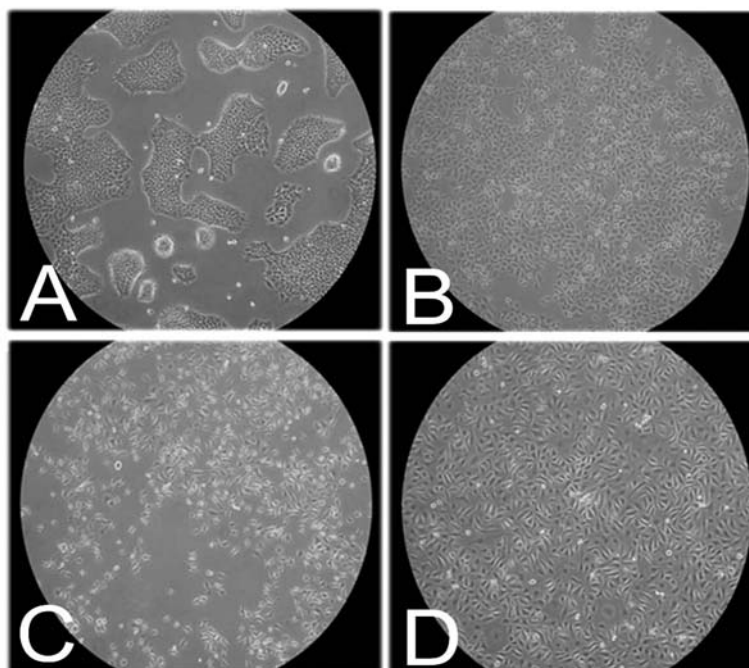


Figure 3. Morphology of SACC83 and ACCh cell lines. The SACC83 (A, B) and ACCh (C, D) cells were grown as monolayers under standard growth conditions of 37°C, 5% CO₂ with DMEM plus 10% FBS or KGM and photographed at pre-confluence (A, C) and at confluence (B, D). Note: SACC83 cells are basaloid clusters rich in cell-cell contacts at pre-confluence (A) and then take on a cobblestone appearance at confluence (B). Note: ACCh cells (C, D) retain a spindle-shaped myoepithelial appearance at pre-confluence and confluence.

cell lines. The SACC83 cells represent a well- differentiated, epithelial cell type similar to the cribriform ACC subtype. Whereas, the ACCh cell line represents a poorly-differentiated cell type similar to the solid subtype of ACC

Positive correlation between invasion and $\alpha\beta 6$ integrin expression. A functional assay was done to categorize the cell lines' invasiveness. The two cell lines (ACCh and the SACC83) were evaluated for invasion using the standard Transwell assay. The upper surface of an 8 μ m pore size Transwell filter was coated with a thin layer of Matrigel. Matrigel was allowed to polymerize at 37°C for 1 h in the presence of 5% CO₂. 400 μ l of peritumor fibroblast (PTF) conditioned medium (CM) was placed into the lower chamber to act as a chemoattractant (11). 2 \times 10⁵ cells/ml were placed onto the upper surface of the Matrigel and allowed to invade for 24 h. To evaluate the potential influence that the $\alpha\beta 6$ integrin may have on ACCh cell motility, triplicate wells of ACCh cells were incubated in the presence of the $\beta 6$ function blocking antibody 10D5. Our results show that the ACCh cells were 7-fold more invasive than the SACC83 cell line (Figure 6). When the ACCh cells were incubated in the presence of the $\beta 6$ -function blocking antibody 10D5, invasion was decreased by 50% (Figure 6). These results suggest that the ACCh cells are significantly more invasive than the SACC83 cell line and that this invasion is partially mediated by the $\alpha\beta 6$ integrin.

Discussion

Characteristically, ACC has regional recurrence and distant metastasis to peripheral nerves. As the tumor grows and invades nerves, pain, numbness, paralysis, and death can occur. Distant metastases can develop despite loco-regional tumor control and can occur more than ten years after initial therapy. Ultimately, ACC is a difficult cancer to target and successfully treat due to the low mitotic index of cells but high rate of recurrence and highly invasive nature (11). Therefore, a better understanding of the biology of ACC would permit the development of more effective therapeutic approaches.

Prognosis for ACC is dependent upon on the presenting growth pattern: cribriform, tubular, or solid. The cribriform subtype has the best prognosis, whereas the solid growth type is associated with the poorest patient outcome. Identifying the process that results in the transition from the cribriform to solid growth pattern could be a target for long-term treatment of this disease. In this study, we determined characteristics of ACC described for the first time. We suggest that the aggressive behavior of the ACC tumors and the cribriform to solid subtype switching is a modification of EMT. The $\alpha\beta 6$ integrin is a major contributor to epithelial tumor invasion and was highly expressed in the solid subtype. The tissue sections also revealed a dramatic increase in the expression of TN-C when analyzed by



Figure 4. E-cadherin and vimentin expression in SACC83 and ACCh cell lines. SACC83 and ACCh cells were seeded serum-free and grown for 24 h at 37°C in 5% CO₂. The cells were lysed and evaluated by western blotting using antibodies against E-cadherin (clone She-78-7) or vimentin (clone 3B4). Cell lysates were separated by SDS-PAGE and subjected to western Blotting using antibodies against E-Cadherin (A) and vimentin (B). Antibodies against actin (mAb 3128) were used as a loading control. Relative value units (rvu) were assigned using dosimetry.

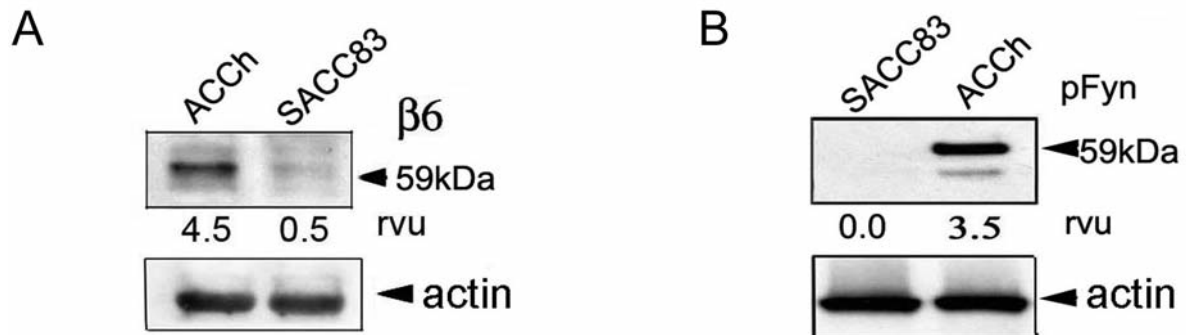


Figure 5. $\alpha v \beta 6$ integrin and pFyn expression in SACC83 and ACCh cell lines. The cells were grown serum-free overnight and then were lysed. The lysates from SACC83 and ACCh cell lines were evaluated for the expression of $\alpha v \beta 6$ integrin (A) and Fyn kinase (B). Cell lysates were separated by SDS-PAGE and subjected to western Blotting using monoclonal antibodies against $\alpha v \beta 6$ integrin (A) and Fyn (B). Antibodies against actin (mAb 3128) were used as a loading control. Relative value units (rvu) were assigned using dosimetry.

immunohistochemistry. The expression of the $\alpha v \beta 6$ integrin and TN-C in the solid form but not in the cribriform subtype suggests that the transition is a result of EMT. Perhaps the indolent nature of the cribriform type may be in part due to its highly differentiated state when compared with the poorly-differentiated solid state. The $\alpha v \beta 6$ integrin and TN-C have been implicated in EMT and poor prognosis in colon carcinoma cells as well as in oral squamous cell carcinoma.

We defined the specific characteristics in two ACC cell lines: SACC83 and ACCh. Differences in growth characteristics were apparent. The SACC83 cells tended to grow in basaloid, epithelial-like colonies and then progressed to a cobblestone-like appearance at confluence, which is reminiscent of cribriform morphology. In contrast, the ACCh cells grew as individual spindle-type cells and had a myofibroblast-type appearance, which is similar to the solid subtype. The morphological appearance of the two cell lines corresponded to the expression of E-cadherin and vimentin; which are established markers of the epithelial and

mesenchymal phenotype, respectively. The nesting appearance demonstrated by the SACC83 cells is directly associated with the high E-cadherin expression whereas the spindle shaped mesenchymal morphology of the ACCh cells corresponded to the minimal expression of E-cadherin. Additionally, the ACCh cell line expressed the higher levels of the $\alpha v \beta 6$ integrin and phosphorylated Fyn kinase, which are known promoters of EMT. We have previously shown that Fyn forms a complex with the $\beta 6$ cytoplasmic tail of the $\alpha v \beta 6$ integrin and initiates EMT through activating the FAK/RAS/MAPK/MMP3 signaling pathway (12). Lastly, the in vitro invasive potential of SACC83 and ACCh cells was examined. The $\alpha v \beta 6$ integrin-expressing ACCh cell line was approximately 7-fold more invasive than the SACC83 cell line, when analyzed using a Matrigel invasion assay. Cell invasion was decreased by 50% when incubated with anti- $\beta 6$ antibodies. Our work suggests that one major difference between the cribriform and the solid form is differentiation. The switch is a result of EMT which occurs over time and we suggest this is the reason for the poor

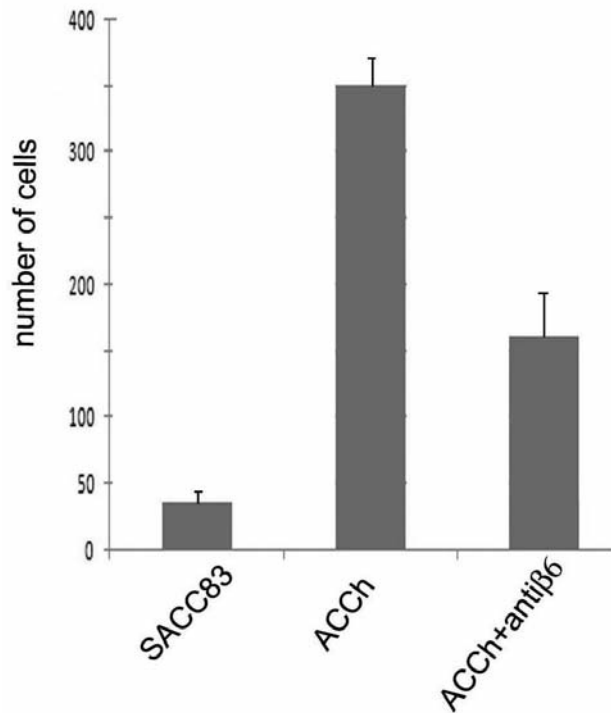


Figure 6. Invasive potential and expression of the $\alpha\beta6$ integrin in SACC83 and ACCh cell lines. Transwell filters (8- μ m pore size) were coated with a thin layer of Matrigel and allowed to polymerize at 37°C for 1 h. A total of 2×10^5 cells/ml were plated onto each Matrigel-coated membrane. 400 μ l of fibroblast (PTF)-conditioned medium (CM) was placed into lower chamber as a chemo-attractant. The cells were allowed to migrate for 24 h. The experiment was terminated, by fixing the cells in crystal violet. The upper surface was wiped clean and the number of cells traversing the membrane was determined. The $\beta6$ -positive ACCh cells were also incubated in the presence of 10 μ g/ml of $\beta6$ -function blocking antibody 10D5. Note that the invasion of ACCh cells can be partially inhibited using the anti- $\beta6$ antibody 10D5.

prognosis of the disease. Understanding the time frame when specific signals are generated and what environmental cues are deemed essential will be of great help in designing future therapeutic reagents.

Acknowledgements

This work was supported by a grant from the University of California, Cancer Research Coordinating Committee and by the generous support of the Department of Orofacial Sciences, UCSF.

References

- Gondivkar SM, Gadbail AR, Chole R and Parikh RV: Adenoid cystic carcinoma: a rare clinical entity and literature review. *Oral Oncol* 4: 231-236, 2011.
- Ishii K, Shimoda M, Sugiura T, Seki K, Takahashi M, Abe M, Matsuki R, Inoue Y and Shirasuna K: Involvement of epithelial-mesenchymal transition in adenoid cystic carcinoma metastasis. *Int J Oncol* 4: 921-931, 2011.
- West RB, Kong C, Clarke N, Gilks T, Lipsick JS, Cao H, Kwok S, Montgomery KD, Varma S and Le QT: Myc expression and translocation in adenoid cystic carcinomas and other salivary gland tumors with clinicopathologic correlation. *Am J Surg Pathol* 35: 92-99, 2011.
- Ellis GL and Auclair PL: Tumors of the salivary glands. *Atlas of Tumor Path* pp. 225-259, 2008.
- Da Cruz Perez DE, De Abreu Alves F, Nobuko N, De Almeida OP and Kowalski LP: Prognostic factors in head and neck adenoid cystic carcinoma. *Oral Oncol* 42: 139-146, 2006.
- Bates RC: Colorectal cancer progression: integrin $\alpha\beta6$ and the epithelial-mesenchymal transition (EMT). *Cell Cycle* 4: 1350-1352, 2005.
- Munger JS, Huang X, Kawakatsu H, Griffiths MJ, Dalton SL, Wu J, Pittet JF, Kaminski N, Garat C, Matthey MA, Rifkin DB and Sheppard D: The integrin $\alpha\beta6$ binds and activates latent TGF beta 1: a mechanism for regulating pulmonary inflammation and fibrosis. *Cell* 96: 319-328, 1999.
- Murphy-Ullrich JE, Lightner VA, Aukhil I, Yan YZ, Erickson HP and Hook M: Focal adhesion integrity is downregulated by the alternatively spiced domain of human tenascin. *J Cell Biol* 115: 1127-1136, 1991.
- Ramos DM, Dang D and Sadler S: The role of the integrin $\alpha\beta6$ in regulating the epithelial to mesenchymal transition in oral cancer. *Anticancer Res* 29: 125-130, 2009.
- Perzin KH, Gullane P and Clairmont AC: Adenoid cystic carcinomas arising in salivary glands: a correlation of histologic features and clinical course. *Cancer* 42: 265-282, 1978.
- Dang D, Yang Y, Li X, Atakilit A, Regezi J, Eisele D, Ellis D, Ramos DM: Matrix metalloproteinase's and TGFbeta1 modulate oral tumor cell matrix. 316:937-942, 2004.
- Zhang Y, Wang J, Dong F, Li H and Hou Y: The effect of proteoglycans inhibited on neurotropic growth of salivary adenoid cystic carcinoma. *J Oral Pathol Med* 40: 476-482, 2011.
- Dang D, Bamburg JR and Ramos DM: $\alpha\beta6$ integrin and cofilin modulate K1735 melanoma cell invasion. *Exp Cell Res* 312: 468-477, 2006.

Received July 16, 2012

Accepted July 16, 2012